Expansion and mechanistic insights into de novo DEAF1 variants in DEAF1-associated neurodevelopmental disorders

McGee, S.R.; Rajamanickam, S.; Adhikari, S.; Falayi, O.C.; Wilson, T.A.; Shayota, B.J.; ... ; Jensik, P.J.

OXFORD

Human Molecular Genetics, 2023, Vol. 32, 3, 386–401
https://doi.org/10.1093/hmg/ddac200
Advance access publication date 18 August 2022
Original Article

Expansion and mechanistic insights into *de novo* DEAF1 variants in *DEAF1*-associated neurodevelopmental disorders

Stacey R. McGee[1], Shivakumar Rajamanickam[1], Sandeep Adhikari[1], Oluwatosin C. Falayi, Theresa A. Wilson[12], Brian J. Shayota[12,13], Jessica A. Cooley Coleman[2], Cindy Skinner[2], Raymond C. Caylor[2], Roger E. Stevenson[2], Caio Robledo D' Angioli Costa Quaio[3,4], Berenice Cunha Wilke[5], Jennifer M. Bain[6], Kwame Anyane-Yeboa[7], Kaitlyn Brown[8], John M. Greally[8,9], Emilia K. Bijlsma[10], Claudia A.L. Ruivenkamp[10], Keren Politi[11], Lydia A. Arbogast[1], Michael W. Collard[1], Jodi I. Huggenvik[1], Sarah H. Elsea[12] and Philip J. Jensik[1,*]

[1]Department of Physiology, Southern Illinois University School of Medicine, Carbondale, IL USA
[2]Greenwood Genetic Center, Greenwood, SC, USA
[3]Instituto da Criança (Children's Hospital), Hospital das Clínicas (HCFMUSP), Faculdade de Medicina (FMUSP), Universidade de São Paulo, São Paulo, SP, Brazil
[4]Laboratório Clínico, Hospital Israelita Albert Einstein, São Paulo, SP, Brazil
[5]Unicamp, Campinas, SP, Brazil
[6]Department of Neurology, Division of Child Neurology, Columbia University Irving Medical Center, New York, USA
[7]Department of Pediatrics, Division of Clinical Genetics, Columbia University Irving Medical Center, New York, USA
[8]Departments of Pediatrics and Genetics, Albert Einstein College of Medicine, Bronx, NY USA
[9]Departments of Genetics, Albert Einstein College of Medicine, Bronx, NY USA
[10]Department of Clinical Genetics, Leiden University Medical Centre, PO box 9600, 2300 RC, Leiden, The Netherlands
[11]ALYN Hospital, Jerusalem, Israel
[12]Department of Molecular and Human Genetics, Baylor College of Medicine, Houston, USA
[13]Department of Pediatrics, Division of Genetics, University of Utah, Salt Lake City, UT
*To whom correspondence should be addressed at: Southern Illinois University School of Medicine, 1135 Lincoln Drive, Carbondale, IL 62901, USA. Tel: 618-453-1525; Fax: 618-453-1527; Email: pjensik@siumed.edu

Abstract

De novo deleterious and heritable biallelic mutations in the DNA binding domain (DBD) of the transcription factor deformed epidermal autoregulatory factor 1 (DEAF1) result in a phenotypic spectrum of disorders termed *DEAF1*-associated neurodevelopmental disorders (DAND). RNA-sequencing using hippocampal RNA from mice with conditional deletion of *Deaf1* in the central nervous system indicate that loss of *Deaf1* activity results in the altered expression of genes involved in neuronal function, dendritic spine maintenance, development, and activity, with reduced dendritic spines in hippocampal regions. Since *DEAF1* is not a dosage-sensitive gene, we assessed the dominant negative activity of previously identified *de novo* variants and a heritable recessive *DEAF1* variant on selected DEAF1-regulated genes in 2 different cell models. While no altered gene expression was observed in cells over-expressing the recessive heritable variant, the gene expression profiles of cells over-expressing *de novo* variants resulted in similar gene expression changes as observed in CRISPR-Cas9-mediated *DEAF1*-deleted cells. Altered expression of DEAF1-regulated genes was rescued by exogenous expression of WT-DEAF1 but not by *de novo* variants in cells lacking endogenous DEAF1. *De novo* heterozygous variants within the DBD of DEAF1 were identified in 10 individuals with a phenotypic spectrum including autism spectrum disorder, developmental delays, sleep disturbance, high pain tolerance, and mild dysmorphic features. Functional assays demonstrate these variants alter DEAF1 transcriptional activity. Taken together, this study expands the clinical phenotypic spectrum of individuals with DAND, furthers our understanding of potential roles of DEAF1 on neuronal function, and demonstrates dominant negative activity of identified *de novo* variants.

Introduction

Intellectual disability (ID), one of the common neurodevelopmental disorders with an estimated prevalence of about 1–3%, has a strong genetic component, and yet, the pathogenesis of non-inherited versions of non-syndromic ID is poorly understood (1–3). Deformed Epidermal Autoregulatory Factor 1 (DEAF1, MIM 602635) is a transcription factor that is expressed at increased levels in the central nervous system and is highly conserved across species (4,5). DEAF1 has multiple functional domains and has been implicated in a myriad of diseases, including autoimmune disorders like type 1-diabetes mellitus, altered serotonergic signaling through *HTR1A* gene dysregulation, and major depressive disorder (6–10). *DEAF1*-associated neurodevelopmental disorder (DAND, MIM 602635, 615 828, 617 171) is a an autism spectrum disorder with ID, a spectrum of neurobehavioral characteristics, and seizures (11–13) associated with either a heterozygous *de novo* variant or biallelic heritable variants in *DEAF1*. Both the autosomal dominant and recessive forms have been described

Received: May 13, 2022. **Revised:** July 11, 2022. **Accepted:** August 8, 2022

with a similar phenotypic spectrum (14–16). Currently, increased prevalence of brain abnormalities is the only difference between heritable and de novo forms (13).

Unlike the identified recessive *DEAF1* variants, the *de novo* single allelic variants cluster within the DNA binding domain (DBD) of DEAF1 (13). Functional studies indicate these variants can inhibit DEAF1 transcriptional function, DNA binding, or alter cellular localization. *DEAF1* is not a dosage-sensitive gene, as individuals with a single *DEAF1* gene do not display a phenotype. However, DEAF1 dimerizes with itself through the DBD or a downstream nuclear export signal containing a coiled-coiled domain (17) and because of these DEAF1-DEAF1 protein interaction domains, it is possible *de novo* DEAF1 mutant proteins have dominant negative actions on wild-type DEAF1 function (13).

Whole animal *Deaf1* deletion in mice results in neural tube defects and perinatal lethality (11,18); whereas mouse models utilizing conditional deletion of *Deaf1* in neuronal precursor cells have shown the importance of DEAF1 activity on neurobehaviors. Loss of *Deaf1* results in significant cognitive deficits, including impaired contextual fear and spatial memory, as well as heightened anxiety-like behaviors (11,19). *Deaf1* conditional deletion also results in altered marble burying activity, potentially due to increased anxiety behavior and decreased hippocampal volume (19). Because DEAF1 is a transcription factor, it is likely that alterations in the expression of DEAF1-regulated genes may result in the phenotype described in mouse models and potentially in DAND.

The importance of DEAF1 in neurodevelopment and cognition is evident, but mechanisms underlying the pathogenesis of DAND are still unclear. In this study, we sought to (1) identify DEAF1-regulated genes by RNA-sequencing using hippocampal RNA from control and *Deaf1* conditional deletion mice, (2) determine if selected DEAF1 variants have dominant negative actions on WT-DEAF1 function, (3) assess alterations in dendritic spine number in hippocampal regions of *Deaf1* conditional deletion mice and (4) functionally assess the effects of newly identified *de novo* variants on DEAF1 transcriptional activity and describe the clinical features of individuals with these variants in *DEAF1*, thereby adding to the description of DAND. The data presented here expand the described clinical phenotype of DAND and provide new insights into DEAF1-regulated genes in the hippocampus and selected brain regions. We also show that *de novo* variants have dominant negative actions on WT-DEAF1 transcriptional function.

Results

Alterations in the transcriptional profile of *Deaf1* NKO hippocampus

Previous studies indicate *Nestin*-cre mediated deletion of *Deaf1* in the central nervous system of mice (termed NKO) results in decreased spatial and contextual fear memory (11,19). To identify Deaf1-regulated genes that may underlie learning and memory alterations, RNA-sequencing was performed comparing poly A-enriched mRNA from control and NKO hippocampal tissue. Analysis identified 347 gene transcripts that were significantly differentially expressed (cutoff FDR < 0.05) between control and NKO mice (Fig. 1A and B). Gene ontology analysis (biological function) of the 347 genes displayed an enrichment of genes involved in transport, neuronal differentiation and behavior (Fig. 1C). Gene ontology was also performed on differentially expressed down-regulated genes ($n = 208$) and showed an enrichment for genes important for normal functioning of mature neurons (Fig. 1D). These include intracellular transport, secreted proteins, peptide hormones, regulators of signaling, ion transport, among others. Genes that were up-regulated ($n = 139$) in NKO mice clustered around developmental processes such as neurogenesis, neuronal differentiation and maturation, morphogenesis, and to some extent, genes important for transport of neurotransmitters to terminals and signaling (Fig. 1E). *In silico* analysis of the mouse genome indicates the DEAF1 consensus sequence TCG(N5-N11)TCG is found in the promoter sequences (−3000 bp to −1 bp upstream of transcription start site) of 128 of the 347 identified genes (using RSA-Tools Genomic Scale PatternSearch (20)). The differentially expressed genes identified in this study are likely a combination of genes directly regulated by DEAF1 and others are the result of altered downstream pathways due to a loss of DEAF1 activity (indirect DEAF1 actions). Several differentially expressed genes identified by RNA-seq were confirmed by RT-qPCR using hippocampal RNA from control and NKO mice. We found strong correlation in the magnitude of change, in both up- and down-regulated gene transcripts, between qPCR expression levels and fold-change reported by RNA-seq (Supplementary Material, Fig. S1). Similar effects on gene expression were confirmed by RT-qPCR experiments performed using RNA isolated from frontal cortex, cerebellum and striatum (Supplementary Material, Fig. S2).

DEAF1 regulation of *UBE2M*

Ube2m (identified as a DEAF1-regulated gene) is part of the neddylation pathway and has described roles in the regulation of dendritic spines (21). Sequence analysis indicates a putative DEAF1 consensus sequence in the proximal promoter in both mouse and human *UBE2M* genes (Fig. 2A). EMSA was performed with either purified wildtype DEAF1 or the previously identified DEAF1 variant, p.Gln264Pro, protein using dsDNA probes for 6spcon or a probe containing the consensus sequence from *Ube2m* (Fig. 2B). DEAF1 bound to the putative *Ube2m* DEAF1 consensus sequence, but DNA binding was not observed for p.Gln264Pro. To further confirm DEAF1 binding to the *Ube2m* proximal promoter, ChIP was performed using hippocampal tissue from control and NKO mice. DEAF1 was previously shown to bind its own promoter (Fig. 2C). Compared to pre-immune controls, DEAF1 was significantly enriched at the *Deaf1* promoter in hippocampal tissue. DEAF1 was not enriched at the *Deaf1* promoter in NKO mice, demonstrating both loss of DEAF1 in NKO and specificity of the DEAF1 antibody in ChIP experiments. Compared to pre-immune controls, DEAF1 was significantly enriched at the proximal promoter of *Ube2m*-containing the putative DEAF1 consensus sequence. Again, enrichment was not observed in NKO hippocampal tissue. UBE2M protein levels were determined by western blot analysis using proteins isolated from the hippocampi of control and NKO mice (Fig. 2D). A significant decrease in UBE2M was observed in the hippocampi of NKO mice.

DEAF1 transcriptional regulation of *UBE2M* was also observed in the human cell line HEK293T. RT-qPCR was performed on selected genes identified by RNA-seq in control HEK293T (293 T control) and CRISPR-Cas9-mediated *DEAF1* deletion in HEK293T (293 T *DEAF1*-KO) cells. Compared to 293 T control cells, *UBE2M* and *B4GAT1* were significantly decreased and *RABEP2* was significantly increased in 293 T *DEAF1*-KO cells (Fig. 3A). UBE2M protein levels were determined by western blot analysis, comparing 293 T control 293 T *DEAF1*-KO cells (Fig. 3B). A significant decrease in UBE2M was observed in 293 T *DEAF1*-KO cells. ChIP was also performed to demonstrate binding of DEAF1 to the *UBE2M* proximal promoter. DEAF1 was bound to its own promoter and the *UBE2M* promoter in 293 T control cells. No binding was shown at the downstream negative control exon 6 region of *DEAF1*. No binding

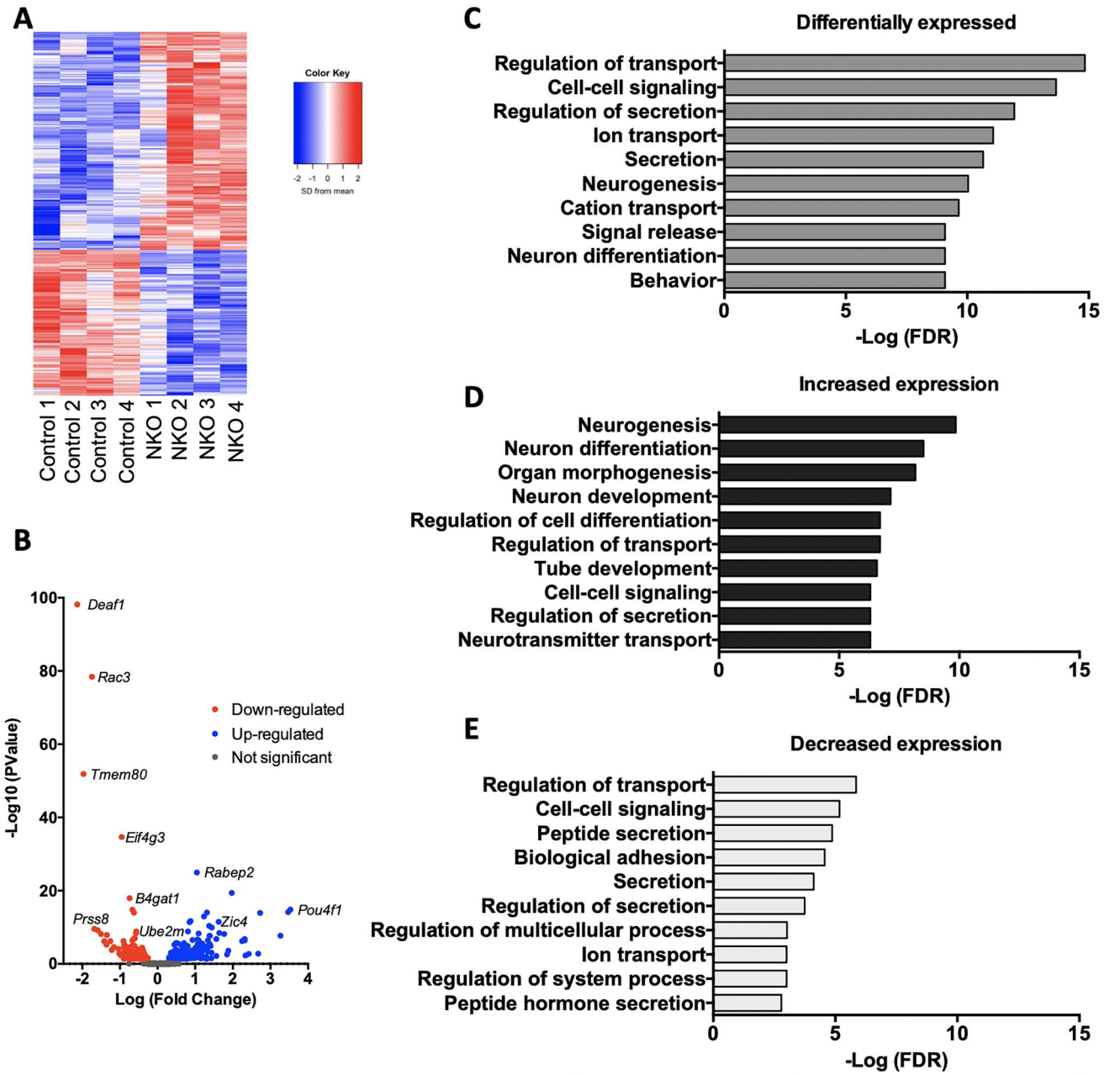

Figure 1. Transcriptomic changes in the hippocampus of NKO mice highlight Deaf1 role in neuronal function. (**A**) Heat map and (**B**) volcano plot of the 347 identified differentially expressed genes (red color indicates decreased expression and blue indicates increased expression) by RNA-sequencing using hippocampal RNA from 4 control and 4 NKO mice. Biological function enrichment analysis of (B) all 347 genes, (**C**) genes with increased expression and (**D**) genes with decreased expression.

was observed at any of the sequences in 293 T *DEAF1*-KO cells, demonstrating deletion of *DEAF1* (Fig. 3C).

Effects of DEAF1 function on dendritic spine in the mouse hippocampus

Since DEAF1 is important for learning and memory and regulates *Ube2m* expression, as well as other genes involved in neuronal maturation, we sought to determine if decreased DEAF1 activity would affect dendritic spine formation in the hippocampus comparing control, Het and NKO mice. Golgi-Cox staining allowed for visualization of dendritic spines and were counted per unit length (μm) (Fig. 4A). No changes in dendritic spine number were observed in apical or basal CA1 neurons in control, Het, or NKO mice (Fig. 4B). However, a significant decrease in spine number was observed in CA3 basal region in NKO mice compared to control but with no changes observed in the CA3 apical region (Fig. 4C). Significant decreases in total spine number in NKO mice were observed in the dentate gyrus (DG) in both proximal and distal regions (Fig. 4D).

Dominant negative activity of *de novo* DEAF1 variants

The variant p.Arg226Trp is a heritable bi-allelic variant, identified in several individuals (12,14,16). Individuals with a single p.Arg226Trp do not display a DAND spectrum phenotype, as evidenced by phenotypically normal carrier parents and is

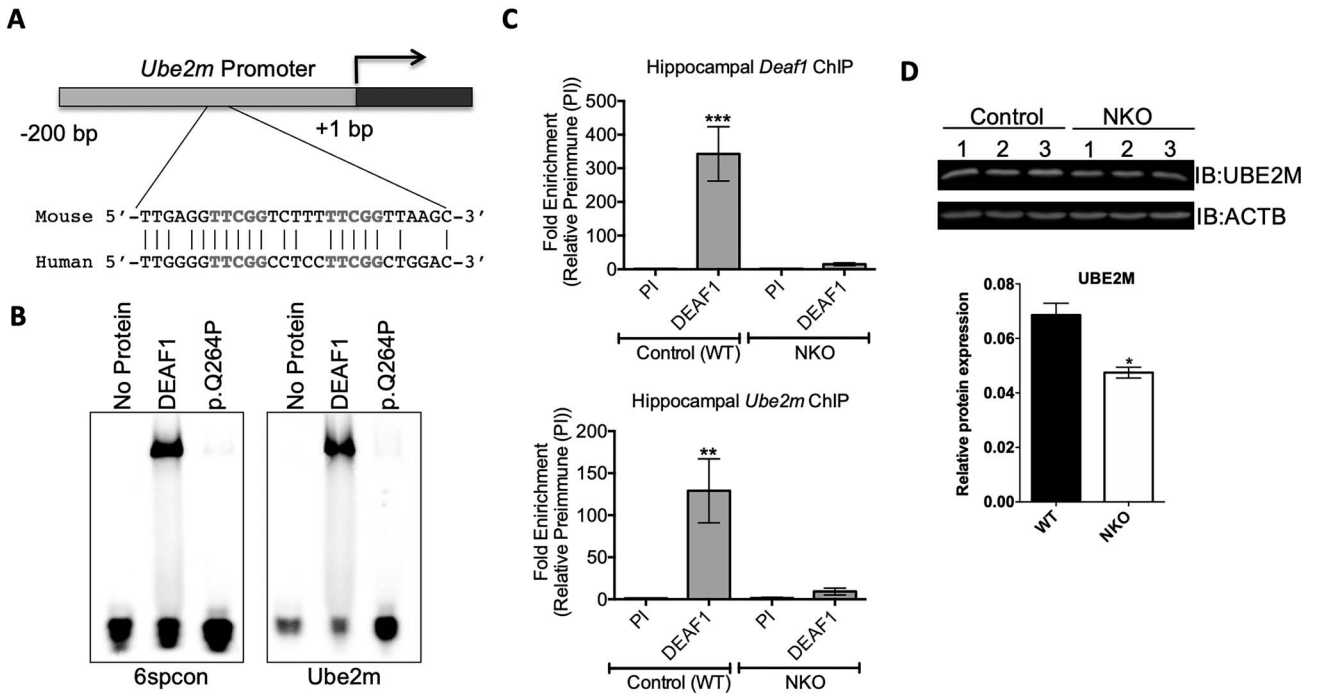

Figure 2. DEAF1 regulation of *UBE2M*. (**A**) Location and sequence of a putative DEAF1 consensus sequence within the *UBE2M* proximal promoter. Both mouse and human sequences are shown. (**B**) EMSA using WT or p.Q264P DEAF1 proteins with control 6spcon or *Ube2m* dsDNA probes. (**C**) ChIP was performed using hippocampal tissue from control or NKO mice with pre-immune serum (PI) or anti-DEAF1 antibodies. Quantitative PCR was performed using primers designed to amplify a known DEAF1 binding region within the *Deaf1* promoter or the *Ube2m* proximal promoter. Each bar represents mean +/− SEM fold enrichment relative to control PI ($N = 3$). **$P < 0.01$ using one-way analysis of variance followed by Dunnett's multiple comparisons test (versus control PI). (**D**) Western blots were performed on hippocampal tissue from control or NKO mice using anti-UBE2M and anti-ACTB antibodies. Each bar represents mean +/− SEM relative to ACTB expression for each animal ($N = 3$). *P,0.05 using Student's *t*-test.

not expected to display dominant negative activity. Individuals carrying the heterozygous *de novo* variant c.664 + 1G > T that results in exon 4 skipping and an in-frame deletion within the SAND domain (p.Pro174_Gly222del), or the *de novo* missense variant, p.Gln264Pro, display the DAND phenotype have been previously described (11,13). To determine if identified heritable or *de novo* DEAF1 variants affect the expression of 3 of the identified DEAF1-regulated genes (*UBE2M*, *B4GAT1* and *RABEP2*), HEK293T cell lines, which endogenously express *DEAF1*, were generated that stably express GFP, DEAF1, p.Arg226Trp, p.Pro174_Gly222del and p.Gln264Pro. Stable cell lines showed nuclear localized DEAF1, as well as over-expression of the indicated variant (Fig. 5A and B). *DEAF1* mRNA expression increased around 2-fold in DEAF1-variant stable cell lines compared to control GFP-expressing cells (Fig. 5C). The stable cells expressing *de novo* variants, p.Pro174_Gly222del and p.Gln264Pro, had significantly reduced *B4GAT1* and significantly increased *RABEP2* expression compared to control and DEAF1 cells (Fig. 5D and E). *UBE2M* mRNA was only significantly reduced in p.Gln264Pro cells, but there was a decreasing trend in p.Pro174_Gly222del cells (Fig. 5F). No change in DEAF1-regulated gene expression was observed for the heritable p.Arg226Trp variant. UBE2M protein levels were decreased in both p.Pro174_Gly222del and p.Gln264Pro cells but not in the heritable variant p.Arg226Trp cells (Fig. 5G). Taken together only cells expressing *de novo* variants had altered expression of DEAF1-regulated genes likely indicating dominant negative activity on endogenous DEAF1 function.

Similar experiments were performed in HEK293T stable cells expressing other previously described *de novo* variants p.Gly212Ser, p.Arg224Trp, p.Ile228Ser, p.Trp234Arg, p.Arg246Thr and p.Arg254Ser (Supplementary Material, Fig. S3). These experiments included a DEAF1-DEAF1 interaction domain double mutant p.His275Ser-del447–475 (17). This double mutant eliminates DEAF1-DNA interaction, as well as both DEAF1-DEAF1 protein interaction domains. Compared to control cells, the *de novo* variants again significantly decreased *B4GAT1* and *UBE2M* and increased *RABEP2* expression. No significant alterations in the expression of *B4GAT1*, *RAPEB2* or *UBE2M* were observed for p.His275S-del447–475 expressing cells (Supplementary Material, Fig. S3). The loss of DEAF1-DEAF1 protein interactions eliminates dominant negative activity. Compared to control cells, in cells over-expressing variant p.Ser130_Leu290del, significantly decreased *B4GAT1* and *UBE2M* and increased *RABEP2* expression was observed.

To further demonstrate that dominant negative activity of the p.Gln264Pro variant is due to actions of mutant protein on endogenous DEAF1, HEK293T or CRISPR-Cas9 HEK293T-*DEAF1* KO (homozygous deletion) cells were transduced with AAV particles that express GFP, DEAF1, or the *de novo* p.Gln264Pro variant. Compared to GFP-transduced HEK293T control cells (contain endogenous DEAF1), *UBE2M* and *B4GAT1* expression levels were decreased and *RABEP2* expression was increased in GFP-transduced 293 T-*DEAF1* KO cells (Fig. 6A), again demonstrating that loss of DEAF1 affects the expression of these genes. Transduction of 293 T-DEAF1 KO cells with AAV particles that express WT-DEAF1 resulted in rescue of expression levels of *UBE2M* and *B4GAT1* (trending *RABEP2*) compared to 293 T-Control cells transduced with GFP. Transduction of HEK293T control cells (contain endogenous DEAF1) with AAV particles that express p.Gln264Pro resulted in decreased expression of *UBE2M* and

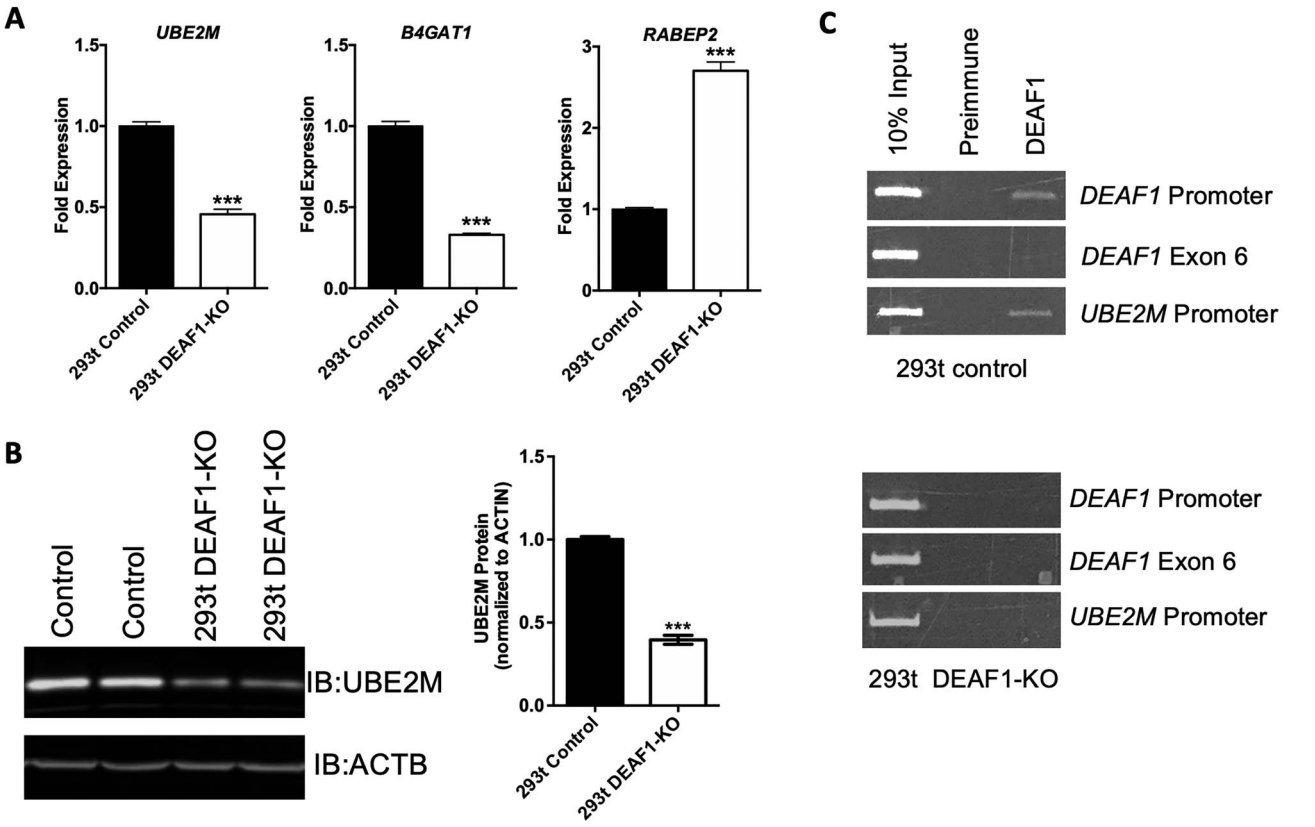

Figure 3. CRISPR/Cas9-mediated deletion of *DEAF1* in HEK293T cells. (**A**) RT-qPCR was performed using RNA isolated from 293 T Control and 293 T *DEAF1*-KO cells to determine changes in the expression of the indicated DEAF1-regulated genes. (**B**) Western blots were performed on proteins isolated from 293 T Control and 293 T *DEAF1*-KO cells using anti-UBE2M and ACTB antibodies. Each bar represents mean +/− SEM relative to control expression ($N = 3$). ***$P < 0.001$ using Student's *t*-test. (**C**) ChIP was performed on 293 T control and 293 T *DEAF1*-KO (CRISPR/Cas9) using pre-immune serum or anti-DEAF1 antibodies. Regions of genomic DNA were amplified using the primers to *DEAF1* promoter (positive control), *DEAF1* Exon 6 (negative control) or *UBE2M* promoter. PCR products were separated on agarose gels.

B4GAT1 and increased expression of *RABEP2*. The expression of *B4GAT1*, *UBE2M*, or *RABEP2* was not altered in 293 T-DEAF1 KO cells transduced with AAV particles that express p.Gln264Pro compared to GFP-transduced 293 T-DEAF1 KO cells. The *de novo* variant p.Gln264Pro only alters expression of DEAF1-regulated genes only if endogenous DEAF1 is present indicating dominant negative activity of the variant on WT-DEAF1 function.

Functional assessment of identified DEAF1 variants

Heterozygous missense *de novo* variants in *DEAF1* were identified in 10 unrelated individuals (Fig. 7). Five of these variants (NP_066288.2:p.Ser221Leu, NP_066288.2:p.Thr238Pro, NP_066288.2:p.Lys250Glu, NP_066288.2:p.Trp252Arg and NP_066288.2:p.Ile256Ser) occur within the SAND domain, while 2 variants occur downstream of the SAND domain but are still located within the DNA binding domain, aa176–306 (NP_066288.2:p.Val294Leu and NP_066288.2:p.Phe297Ser). An additional variant, p.His275Gln (identified as a heterozygous *de novo* variant), was included in this study, and although a complete detailed case report was not available, the individual was referred to the clinic due to global developmental delay, hypotonia and autism spectrum disorder (Table 1). Two of these SAND domain variants, NP_066288.2:p.Lys250Glu and NP_066288.2:p.Trp252Arg, are located in the KDWK motif, which is predicted to contact DNA (22). The variant p.His275Gln occurs at a potential zinc binding motif within the DNA binding domain. In silico prediction analysis using PolyPhen2 and/or SIFT suggest that the variants are likely damaging to protein function. Only p.Phe297Ser was predicted to be tolerated by SIFT but predicted to be likely damaging by PolyPhen2 analysis.

Two different *de novo* variants were identified in individual 9 (Table 1). Trio genome sequencing was performed and identified a *de novo* NM_021008.4:c.332A > C p.Asp111Ala change in *DEAF1*. Additionally, a *de novo* deletion of exons 3–6 was also identified in *DEAF1* (Supplementary Material, Fig. S1A). In order to determine if these two *de novo* alterations were *in cis* or *in trans*, RT-PCR was performed on mRNA from patient lymphoblastoid cells. Primers were designed to specifically distinguish the deletion-containing and the non-deleted *DEAF1* transcripts. Resulting PCR products were then Sanger sequenced to determine if the *de novo* c.332A > C change in exon 2 was present. Sequence analysis revealed the transcript with the deletion of exons 3–6 also possessed the c.332A > C substitution (Supplementary Material, Fig. S1B). The deletion of exons 3–6 results in an in-frame internal deletion in the DEAF1 protein NP_066288.2:p.Ser130_Leu290del.

Transcriptional functional assays were performed to determine the effects of each variant on DEAF1 transcriptional repression and activation activity. Previous studies have shown that DEAF1 represses its own promoter activity (13). Compared to wt-DEAF1, each of the variants assessed significantly impaired DEAF1 transcriptional autorepression activity, although the effects of p.Val294Leu and p.Phe297Ser on repression of *DEAF1*

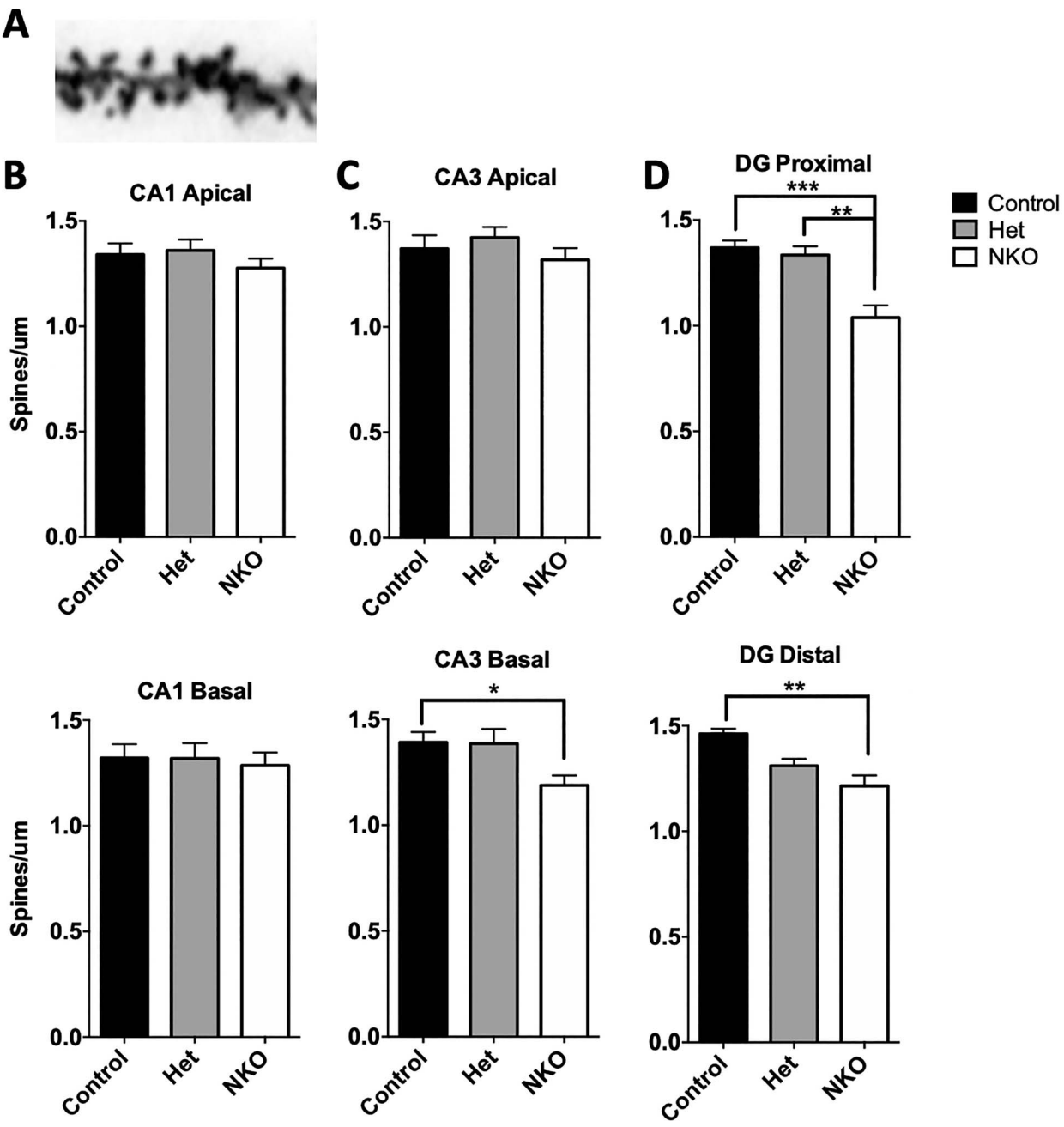

Figure 4. Alterations in dendritic spine number in hippocampal regions of NKO mice. (**A**) Representative image of Golgi-Cox staining (Control) used to visualize neuronal dendritic spines in hippocampal slices of Control, Het and NKO mice. (**B**) Quantification of spine number per μm in apical and basal CA1, apical and basal CA3, and proximal and distal DG regions. Each bar represents mean +/− SEM ($N = 6$ per animal genotype). *P,0.05, **$P < 0.01$ using one-way analysis of variance followed by Bonferroni's multiple comparisons test.

transcription were decreased compared to the other variants (Fig. 8A). We have also shown that DEAF1 enhances *Eif4g3* promoter activity (13). Compared to the approximate 2.5-fold increase in *Eif4g3* promoter activity of wt-DEAF1, p.Ser221Leu, p.Thr238Pro, p.Lys250Glu, p.Trp252Arg, p.Ile256Ser and p.His275Gln suppressed transcriptional activity relative to both *DEAF1* and control pcDNA3 transfected cells. Variants p.Val294Leu and p.Phe297Ser retained transcriptional activation activity (Fig. 8B). The effects of the variants on *DEAF1* transcriptional activity identified in individual 9 were assessed independently. Variant p.Asp111Ala did not alter DEAF1 transcriptional repression or activation activity; however, p.Ser130_Leu290del impaired transcriptional repression activity and suppressed *DEAF1* transcriptional activation activity similar to the previously described p.Gln264Pro variant (Fig. 8C and D).

To further assess the effects of p.Val294Leu and p.Phe297Ser on DEAF1-DNA binding affinity, EMSA was performed using two different double-stranded *DEAF1* DNA consensus binding probes that contain either 6 (6spcon) or 11 (N52–69) bp between the required CG dinucleotides in the half-sites (Fig. 8E). Two additional variants were also included in the analysis, the putative zinc finger variant, p.His275Gln and the previously reported p.Pro293Leu variant (adjacent to p.Val294Leu). Compared to wt-DEAF1, p.His275Gln lost DNA binding; whereas p.Val294Leu,

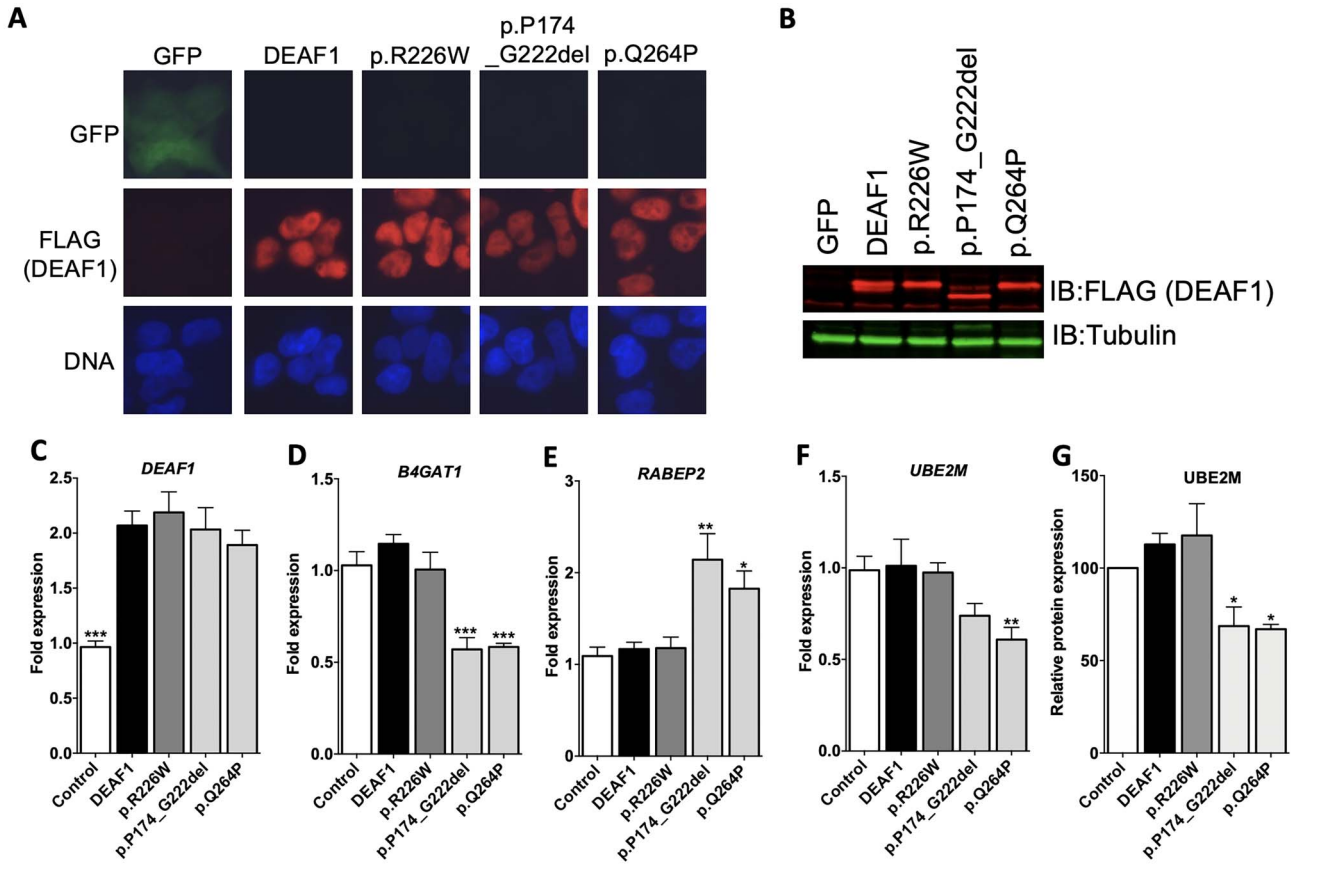

Figure 5. Dominant negative activity of *de novo* DEAF1 variants. (**A**) Immunofluorescent images of 293 T stable cells expressing GFP, WT-DEAF1, or the indicated DEAF1 heritable (p.R226W) or de novo variants (p.P174_G222del, p.Q264P) using anti-FLAG antibodies. (**B**) Western blots were performed on proteins isolated from 293 t stable cells using anti-FLAG (DEAF1) and anti-tubulin antibodies. (**C**) RT-qPCR was performed using RNA isolated from HEK293T Control and HEK293T stable cells to determine changes in the expression of the indicated DEAF1-regulated genes. Each bar represents mean +/− SEM ($N = 4$). $^{*}P < 0.05$, $^{**}P < 0.01$, $^{***}P < 0.001$ compared to DEAF1 using one-way analysis of variance followed by Dunnett's multiple comparisons test.

p.Phe297Ser and p.Pro293Leu displayed a modest reduction in DNA binding affinity for both probes.

Clinical features of individuals with DEAF1 variants

Clinical characteristics of participants ($n = 10$, ages 2–21 y, 50% female) were collated from medical records, as described in the Methods section (Table 1, Fig. 1B). All individuals displayed developmental delays and autism spectrum disorder ($n = 10/10$, 100%). Other findings included regression ($n = 5/10$, 50%), increased pain tolerance ($n = 7/8$, 87.5%), hypotonia ($n = 7/10$, 70%), sleep disturbance ($n = 7/9$, 77.8%), unsteady or ataxic gait ($n = 5/9$, 55.6%), vision or eye problems ($n = 4/7$, 57%) and recurrent infections ($n = 5/9$, 55.6%). Behavioral concerns were frequently reported ($n = 8/9$, 88.9%) and included pica reported in 2 individuals, stereotypies ($n = 7/9$, 77.8%), self-biting ($n = 5/8$, 62.5%) and aggression ($n = 4/9$, 44.4%). A variety of mild dysmorphic features were reported ($n = 7/9$, 77.8%); however, consistent findings were not identified across the cohort, as with previous studies (Table 1). Participant 9 was noted to have additional craniofacial and skeletal differences, with phenotypic overlap to fragile X syndrome, including a long thin face, pointed chin, hypotelorism and a gaunt, thin, body habitus (Table 1, Fig. 1). Seizure activity was frequently noted in this cohort ($n = 7/9$, 77.8%), including febrile seizures ($n = 3/9$, 33%), epilepsy ($n = 5/9$, 55.6%) and abnormal EEG ($n = 7/8$, 87.5). MRI imaging was normal for most individuals ($n = 5/7$, 83%); however, a subtle loss of left hippocampal volume was noted in participant 8 and ventricular asymmetry in participant 10 (Table 1). All seizures were reportedly managed effectively by medication.

Discussion

This study functionally characterizes 10 heterozygous *de novo* *DEAF1* variants and expands the clinical phenotypic spectrum of individuals with *DEAF1*-associated neurodevelopmental disorders. All of the DEAF1 variants in this study impair *DEAF1* transcriptional repression activity. Of the 32 DEAF1 variants that have been functionally assessed for alterations in transcriptional repression activity, 100% showed loss of repression activity (11–13). Functional tests for changes in transcriptional repression activity appear to be a more reliable indicator of loss-of-function pathogenic variants. Of the 28 DEAF1 variants that have been functionally assessed for alterations in transcriptional activation activity at the *Eif4g3* promoter, 22 variants displayed repression-like activity and the other 6 variants either only lost activation activity (p.Arg224Trp, p.Ser239Gly) or retained activation activity (p.Arg254Ser, p.Pro293Leu, p.Val294Leu and p.Phe297Ser) (11,13). In this study, 6 of the 8 described variants occur within the highly conserved SAND domain and resulted in altered transcriptional

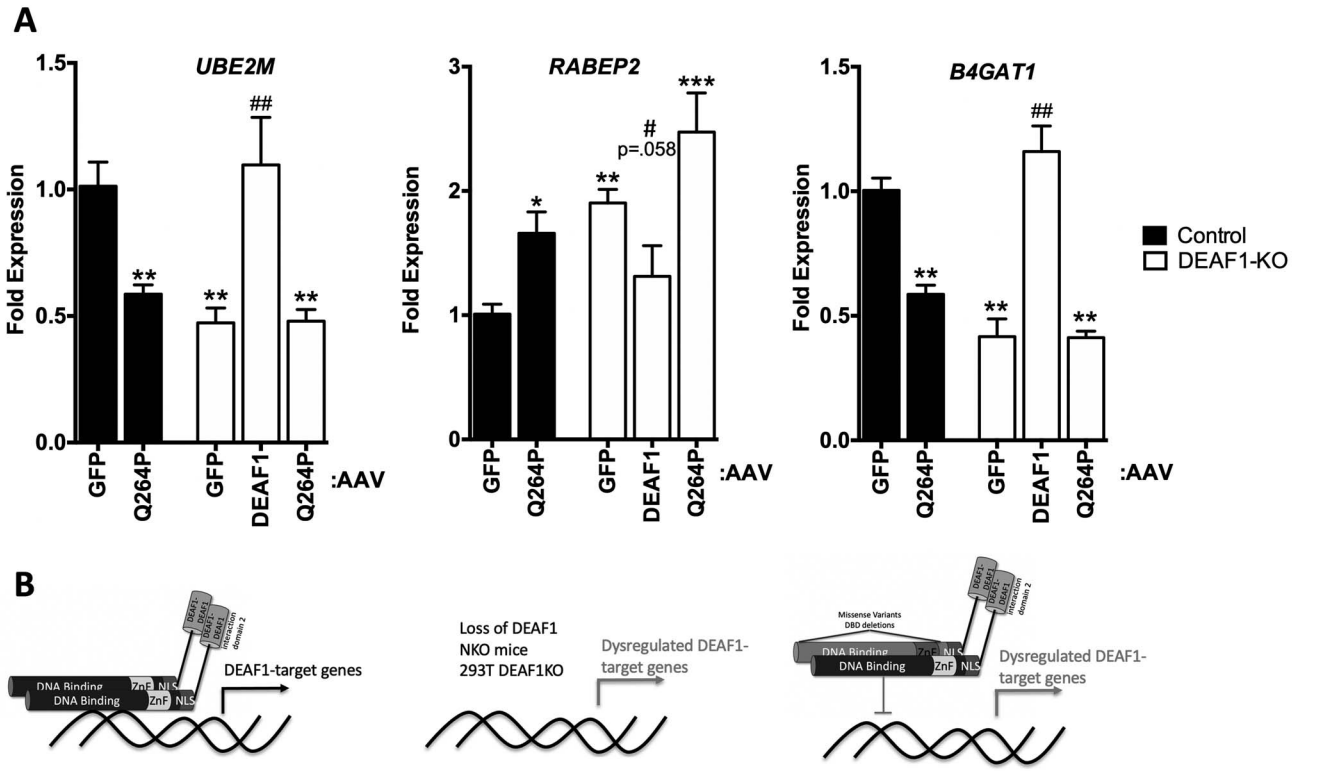

Figure 6. Effects of DEAF1 WT and p.Q264P on DEAF1-regulated gene expression in cells lacking *DEAF1*. (**A**) HEK293T *DEAF1*-KO (CRISPR/Cas9) cells were transduced with AAV particles that express GFP, DEAF1, or DEAF1-p.Q264P. RT-qPCR was performed to determine changes in the expression of the indicated DEAF1-regulated genes. Each bar represents mean +/− SEM (N = 4). *$P < 0.05$, **$P < 0.01$, ***$P < 0.001$ compared to GFP-transduced Control using one-way analysis of variance followed by Fisher's least square comparisons test. #$P < 0.01$ compared to GFP-transduced DEAF1-KO using one-way analysis of variance followed by Fisher's least square comparisons test. (**B**) Models of WT-DEAF1, DEAF1 KO and dominant negative actions of identified DEAF1 variants on DEAF-target gene regulation.

activation activity. The KDWK (DEAF1 aa250–253) motif is proposed to directly contact DNA, and pathogenic variants have been identified at Lys250, Trp252 and Lys253 (22). The variants p.His275Gln and p.Cys279Ser occur at potential zinc coordinating amino acids (23), and p.His275Gln has previously reported in a different individual with DAND (24). We have previously shown that mutation of His275 or Cys279 eliminates both DEAF1-DNA interactions and DEAF1-DEAF1 protein interactions within the DBD (17). The other two variants in this region (p.Val294Leu and p.Phe297Ser) are outside of the SAND domain and resulted in a modest reduction in DNA binding affinity and had no effect on transcriptional activation activity. EMSA indicated DEAF1-DNA interactions were present, albeit reduced relative to wt-DEAF1 for p.Arg254Ser, p.Pro293Leu, p.Val294Leu and p.Phe297Ser (11). A possible explanation for the different effects of the variants on activation activity might be a combination of degree of reduced DNA affinity, as well as altered interactions with other factors that are required for activation activity. Different DEAF1 variants have been shown to have varying effects on interactions with XRCC6 (11), and recently, a de novo splice mutation in *XRCC6* was identified in an individual with ASD (25).

Phenotypically, all of the individuals in this study display developmental delay and autism spectrum disorder, which correspond with the high prevalence described in previous DAND phenotypic descriptions (11–13). Other common features observed including abnormal behaviors, recurrent infections, epilepsy and hypotonia, have been previously described. The descriptions of priapism and elevated lactate levels reported in 2 different individuals in this study have not been previously reported in individuals with *DEAF1* variants and may add to potential phenotypes associated with DAND.

Because DEAF1 is a transcription factor, it is likely that altered cognitive function observed in individuals with *DEAF1* variants is due to changes in DEAF1-regulated genes. Mice with conditional deletion of *Deaf1* in neuronal tissue have reduced contextual fear and spatial memory (11,19). Because these neurobehaviors are attributed, in part, to hippocampal function, we assessed transcriptomic changes in the hippocampus of mice lacking *Deaf1*. Loss of *Deaf1* results in an enrichment of differentially expressed genes that have roles in neuronal function and maturation. Since DEAF1 can function as either a transcriptional activator or repressor, we also assessed gene enrichment by analyzing genes that were upregulated (likely repressed due to DEAF1 function) or downregulated (likely activated due to DEAF1 function). Enrichment in genes important for neurogenesis, neuronal differentiation and development was observed for genes with increased expression. Alterations in these processes have been associated with neurodevelopmental disorders. Developmental gene families were also identified, including Iroquois homeobox (*Irx1–3,5*) and *Zic* family members (*Zic1–5*). Genes with decreased expression were enriched for genes important for neuronal function. Several potassium channel subunits (*Kcnc4*, *Kcne1l*, *Kcng1*, *Kcng4*, *Kcnj10* and *Kcnj4*) and nicotinic receptor subunits (*Chrna3*, *Chrnb3* and *Chrnb4*) were reduced in expression, highlighting potential regulation of neuronal function by DEAF1. Given the high prevalence of seizures and epilepsy in individuals with DAND, further studies could possibly focus on altered potassium channel activity due to changes in expression of these identified subunits (26).

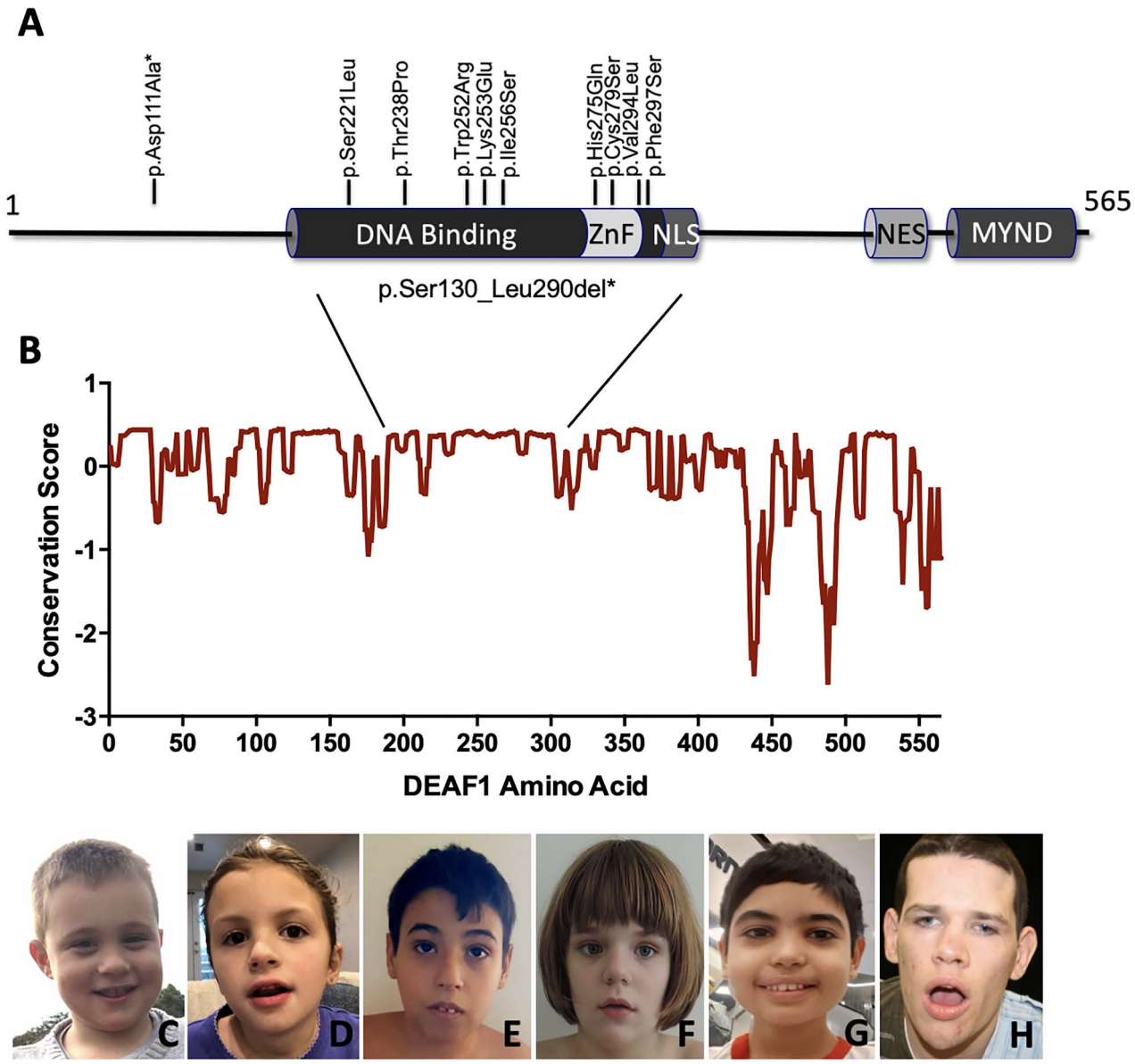

Figure 7. DEAF1 variants and study subjects with *de novo* autosomal dominant *DEAF1*-associated neurodevelopmental disorder (DAND). (A) DEAF1 (Transcript NM_021008.4 and protein NP_066288.2) protein structure including the DNA binding domain (aa173–306), zinc finger region (ZnF), nuclear localization signal (NLS), nuclear export signal (NES) and MYND domain. Also shown are locations of the identified *de novo* heterozygous DEAF1 variants in this study. (**B**) Analysis of conservation of DEAF1 (Consurf) with 14 mammalian homologs, including human DEAF1, using 6 amino acid sliding window. *De novo* DEAF1 variants cluster within the highly conserved DBD. (**C**-**H**) Nonspecific minor facial dysmorphisms are observed, including thick lower lip vermilion, tented upper lip vermilion and pointed chin. (C) Study participant 3 at 8 years of age, heterozygous for the c.712A > C (p.Thr238Pro) variant; (D) study participant 4 at 6 years of age, heterozygous for the c.748A > G (p.Lys250Glu) variant; (E) study participant 5 at 14 years of age, heterozygous for the c.754 T > C (p.Trp252Arg) variant; (F) study participant 6 at 11 years of age, heterozygous for the c.767 T > G (p.Ile256Ser) variant; (G) study participant 7 at 11 years of age, heterozygous for the c.880G > A (p.Val294Leu) variant; (H) study participant 9 at 20 years of age, heterozygous for the c.332A > C (p.Asp111Ala) and deletion of exons 3–6 (GRCh37, g.683978_690053del, p.Ser130_Leu290del).

Overlap between the 2 groups was found for processes such as regulation of secretion. Several similar gene expression changes were observed in other brain areas indicating DEAF1 functional influences are not limited to the hippocampus.

The neddylation pathway is important for dendritic spine development and maturation (21). Inhibition or reduction of the ligase UBE2M alters dendritic spine formation. UBE2M facilitates the conjugation of NEDD8 to the E3 ligase cullin3 (CUL3), and *de novo* variants in *CUL3* have been associated with developmental delays (27). *UBE2M* mRNA and protein expression levels were decreased in the hippocampus, striatum, cerebellum and frontal cortex in mice lacking *Deaf1* and in HEK293T cells lacking *DEAF1*. DEAF1 is bound to the proximal promoter region of *Ube2m* in mouse hippocampus and HEK293T cells. DEAF1 also bound a conserved putative *DEAF1* consensus sequence. Taken together, DEAF1 appears to act as a direct regulator (activator) of *UBE2M* expression. NKO mice had decreased dendritic spine number in the dentate gyrus, and a previous study demonstrated decreased hippocampal volume in these mice (19). Altered dendritic spine density has been observed in mouse models of Angelman syndrome and Rett syndrome; both syndromes have phenotypic overlap with DAND (28,29). Alterations in synaptic development and plasticity may underlie the neurological deficits observed in individuals with DAND. Further studies are needed to

Table 1. Demographic, genomic and phenotypic features of study participants with *DEAF1*-associated neurodevelopmental disorder

Case	1	2	3	4	5	6	7	8	9	10
Age (years)	8	33	8	6	14	11	11	10	21	6
Sex	F	M	M	F	M	F	M	F	M	F
Genomic findings										
Gene	*DEAF1*	*DEAF1*	*DEAF1*	*DEAF1*	*DEAF1*	*DEAF1*	*DEAF1*	*DEAF1*	*DEAF1*	*DEAF1*
HGVS	NM_021008.4	NM_021008.4	NM_021008.4	NM_021008.4	NM_021008.4	NM_021008.4	NM_021008.4	NM_021008.4	NM_021008.4	NM_021008.4
Nucleotide	c.662C > T	c.825C > G	c.712A > C	c.748A > G	c.754 T > C	c.767 T > G	c.880G > A	c.890 T > C	c.332A > C and NC_000011.9 g.683978_690053del; c.563_1045del	c.836G > C
Protein NP_066288	p.Ser221Leu	p.His275Gln	p.Thr238Pro	p.Lys250Glu	p.Trp252Arg	p.Ile256Ser	p.Val294Leu	p.Phe297Ser	p.Asp111Ala and p.Ser130_Leu290del	p.Cys279Ser
DEAF1 domain	SAND	–	SAND	SAND	SAND	SAND	–	–	–	ZnF
Zygosity	heterozygous	heterozygous	heterozygous	heterozygous	heterozygous	heterozygous	heterozygous	heterozygous	Both heterozygous	heterozygous
Inheritance	de novo	de novo	de novo	de novo	de novo	de novo	de novo	de novo	Both de novo	de novo
Phenotype										
Macrocephaly	–	NA	–	+	NA	–	–	+ Progressive	– Microcephaly	–
Dysmorphisms	–	NA	Mild dysmorphic features	Mild macrostomia	Inverted nipples, simplification of earlobes	Mild pectus excavatum	Low hairline, thick eyebrows, long eyelashes, high palate	Leg length asymmetry, early eruption of adult teeth, clinodactyly	Gaunt, asthenic, long limbs, long thin face, hypotelorism, downslanted palpebral fissures, notching of the auricular tragi, short philtrum, prominent lips	–
Autism spectrum disorder	+	+	+	+	+	+	+	+ Poor eye contact	+	+
Developmental delay	+	+	+	+	+	+	+	+	+ Profound	+
Regression	–	–	+ Regression of speech	+	+	–	+	+ Regression of speech at 16 month; nonverbal	–	–
Stereotypic hand movement	–	NA	+ Flapping	–	+ Flapping	+	+	+ Abnormal hand and finger postures	+	+
Self-biting	NA	NA	+	–	+	+	+	–	Uncertain	+
Abnormal behaviors	–	NA	+ Aggression	+ Pica, hyperactivity, aggression, destructive behaviors,	+ Aggression	+ Hyperactive	+ Aggression	+ Pica, flat affect; difficulty producing facial expressions, staring	+ Nonverbal; head banging; self-injurious behaviors	+

Continued

Table 1. Continued.

Case	1	2	3	4	5	6	7	8	9	10
Self- and hetero-aggression	water obsession			Self-aggression when in pain or challenged; no hetero-aggression						
Improved symptoms during fevers	NA	NA	NA	NA	NA	+ developmental skills improvement with fever	+ seizures improve with fever	NA	NA	NA
Sleep disturbance	–	NA	+ Awakens 1-2X nights per week with hyperactivity and agitation	+ Occasional night awakenings with laughter	+ Night terrors from 3–5 y; short sleep (2–3 h per day) without medication	–	+ Night terrors till 2.5 y; awakens 1-4X per night	+ Difficulties falling asleep	+ Awake for 24 h for several days	+
Ataxia or unusual gait	–	NA	–	+	–	–	+	+ Unusual wide-based gait, poor coordination, w/o ataxia	+ Unsteady gait, contractures	+
Increased pain tolerance	+	NA	+	+	+	–	+	+	NA	+ Yes, for wounds; not for bruises
Febrile seizure	–	–	+	–	+	–	–	+	–	–
Epilepsy	–	NA	–	+	–	–	+	+ 4 y staring spells 7 y clonic–tonic 9 y seizure-free	+ 3 days of life	–
Recurrent infections	+ Ear, upper respiratory	NA	+ Upper respiratory infections from 0–2 y (improved after milk withdraw)	+	–	–	–	+ Yeast, ear, throat	+ Ear infections during childhood	–
Vision problems	NA	NA	–	+ Left exotropia	+ Intermittent strabismus	–	+ Intermittent strabismus	+ Abnormal myelination of retinal fibers, severe myopia; partial vision loss in left eye	–	–
Hypotonia	+	+	–	–	+	+ Lower limbs	+	+	–	+
Imaging										
EEG	NA	NA	Disorganized activity	Abnormal, not specified	EEG performed when had febrile seizure; no repeat studies	Normal	Disorganized activity, multifocal epileptic activity with secondary generalization	Rare generalized epileptiform discharges, multifocal rhythmic slowing, diffuse background slowing	Abnormal – not specified	Slow posterior background activity
MRI brain	NA	NA	Normal	Normal	Normal	Normal	Normal	Subtle asymmetric volume loss of the left hippocampus	NA	Mild asymmetry between the lateral ventricles
Other findings	NA	NA	Persistent lactic acidosis	Drooling	NA	NA	Priapism	Constipation, functional abdominal pain, feeding difficulties	Contractures at both knees & right arm; cerebral hemorrhage noted 3 days of life; hyper-reflexive; spasticity	NA

NA = Not available; unknown

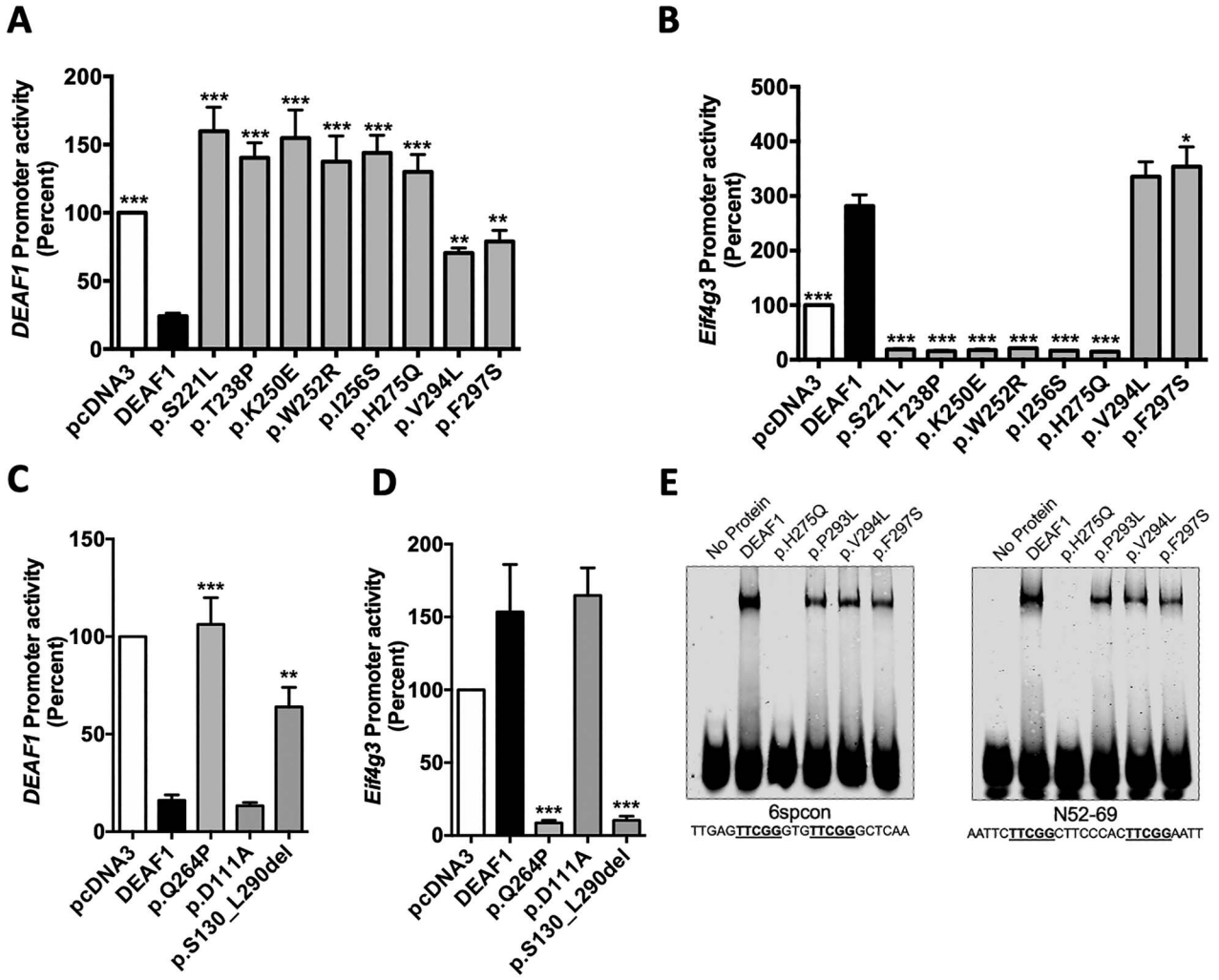

Figure 8. Effects of clinically-identified *DEAF1* variants on DEAF1 transcriptional repression and activation activity. (**A**) and (**C**) HEK293T cells were transfected with *DEAF1* promoter luciferase reporter plasmid with pcDNA3, WT-*DEAF1* or the indicated *DEAF1* variant. DEAF1 repression activity was determined relative to pcDNA3 (set to 100%). (**B**) and (**D**) HEK293T cells were transfected with *Eif4g3* promoter luciferase reporter plasmid with pcDNA3, WT-*DEAF1*, or the indicated *DEAF1* variant. DEAF1 activation activity was determined relative to pcDNA3 (set to 100%). Each bar represents mean +/− SEM ($N = 5$–7 *de novo* variants with $N = 13$ WT for repression studies and $N = 5$ *de novo* variants with $N = 11$ WT for activation studies). *P,0.05, **$P < 0.01$ using one-way analysis of variance followed Dunnett's multiple comparisons test (WT versus each mutant). (**E**) EMSA using WT (DEAF1) or the indicated FLAG-tagged recombinant proteins isolated from transfected HEK293T cells. *DEAF1* consensus dsDNA probes containing 6 bp (6spcon) or 11 bp (N52–69) nucleotides between the CG dinucleotides were examined.

determine the influences of DEAF1 on the neddylation pathway and potential alterations in spine maturation.

Individuals lacking one copy of the *DEAF1* gene do not display a DAND phenotype; thus, haploinsufficiency is not a pathomechanism for *DEAF1*, suggesting further that pathogenic *de novo* DEAF1 variants have dominant negative activity (11). We used two different model systems to demonstrate dominant negative activity of several DEAF1 *de novo* variants. Overexpression of selected identified de novo heterozygous variants in cells containing endogenous WT-DEAF1 resulted in DEAF1-regulated gene expression changes similar to those observed in tissues or cells that lack DEAF1. In addition, a DEAF1 mutant protein that eliminates DEAF1-DNA interactions, and both DEAF1-DEAF1 protein interaction domains within the DBD and downstream NES-containing interaction domain (17) had no dominant negative activity, likely indicating that DEAF1-DEAF1 protein interactions are required for dominant activity. Variant p.Ser130_Leu290del deletes both the DBD and the DEAF1-DEAF1 protein interaction domain contained within the DBD; however, the NES-containing interaction domain remains intact. Interestingly, this variant also displayed dominant negative activity; therefore, it appears the second DEAF1-DEAF1 protein interaction domain containing the NES is required for the dominant negative actions of the mutant DEAF1 proteins on WT-DEAF1 function (potential model assuming DEAF1 dimerization is shown in Fig. 6B). In CRISPR/Cas9-mediated *DEAF1* knockout cells, p.Gln264Pro had no effect on selected DEAF1-regulated gene expression levels. Putative target repressed and activated gene expression levels could be rescued by WT-DEAF1. *De novo DEAF1* variants could only alter DEAF1-regulated gene expression if WT-DEAF1 was present. The heritable bi-allelic variant p.Arg226Trp had no effect on DEAF1-regulated gene expression levels. Previous studies have shown this variant retains DNA binding and transcriptional function. The pathogenic mechanisms underlying this heritable variant might be through alterations in DEAF1-protein interactions or altered (12), not-yet-identified, functions of DEAF1 on cognitive development.

In summary, pathogenic *de novo* variants cause a loss-of-function of DEAF1 activity through reduced or eliminated DNA interactions. Similar alterations in expression of select DEAF1-target genes were observed when comparing cell models lacking *DEAF1* or expressing different identified variants. Therefore, the variants appear to incapacitate WT-DEAF1 protein function through dominant negative actions via DEAF1-DEAF1 protein interactions. The identification of DEAF1-target genes in the hippocampus and other brain regions of mice lacking *Deaf1* allows the connection of DEAF1 to other putative neurodevelopmental disorder causative genes, as well as furthers our understanding of potential roles for DEAF1 in neurogenesis, neurodevelopment and neuronal maturation and function.

Materials and Methods

Plasmid constructs

DEAF1 mammalian expression and *DEAF1* and *Eif4g3* promoter luciferase plasmids have been previously described (11). PCR-mediated site-directed mutagenesis was used to introduce the specific genomic DNA variants into *DEAF1* expression plasmids, derived from the human *DEAF1* complementary DNA (cDNA) (GenBank accession number AF049459). All inserts were confirmed by standard Sanger sequencing.

Transcription assays

Luciferase assays using *DEAF1* and *Eif4g3* promoter luciferase constructs have been previously described (11). HEK293T cells in 24 well plates were transfected with 125 ng pcDNA3 (control) or *DEAF1* (WT or *DEAF1* clinical variants) expression plasmids with 375 ng promoter luciferase and 1.25 ng RSV-Renilla luciferase (normalization) constructs using the calcium phosphate technique for 18 h. Luciferase assays were performed 24 h later using the Dual Luciferase Reporter Assay System (Promega, Madison, WI, USA) on a Biotek Clarity Luminometer.

Electrophoretic mobility shift assay

Epitope FLAG-tagged WT or variant DEAF1 recombinant proteins were purified from transfected human embryonic kidney (HEK293T) cells, as previously described (23). EMSA was performed using the following probes: IRDye800 labeled double-stranded (ds) DNA probe N52–69 (11 space probe) (5,22), IRDye700 labeled probe S6con (6 space probe) (11,17,30), IRDye800 labeled *Ube2m* probe. Recombinant DEAF1 proteins (850 fmol) were incubated with 500 fmol of dsDNA probe and 1 µg of poly(dA–dT) (nonspecific competitor) in a 20 µl reaction containing 70 mM KCl, 35 mM Tris, pH 7.5, 0.7 mM DTT, 2.0% (v/v) glycerol for 20 min at room temperature. Protein–DNA complexes were separated in 4.0% non-denaturing polyacrylamide gels and bands ere visualized on a Li-Cor Odyssey CLx.

Conditional *Deaf1* knockout mice

Generation and breeding of Nestin-cre-mediated conditional *Deaf1* knockout mice have been previously described (11,31). Mice with LoxP sites *f*lanking exons 2–5 of the *Deaf1* gene ($Deaf1^{fl/fl}$) were bred with transgenic $Deaf1^{+/fl;Nes-cre}$ mice, producing mice with conditional homozygous knockout of *Deaf1* ($Deaf1^{fl/fl;Nes\text{-}cre}$, termed NKO), mice with a single *Deaf1* allele and positive for *Nes-cre* ($Deaf1^{+/fl;Nes-cre}$, termed Het) and $Deaf1^{fl/fl}$ mice (termed Control). Mice were maintained in a conventional group-housed colony with a 12 h light, 12 h dark cycle (lights on 0600 h) and fed standard laboratory chow and tap water ad libitum. Male mice 10 month of age or 4 month of age were used for hippocampal tissue collection for RNA-sequencing or Golgi Cox staining, respectively. All experimental work had been approved by the Institutional Animal Care and Use Committee at Southern Illinois University Carbondale.

RNA extraction

Mice were decapitated under deep anesthesia (isoflurane) followed by rapid extraction of brain from the cranium. Hippocampus, striatum, frontal cortex and cerebellum were dissected, flash frozen and total RNA extracted using Trizol (Invitrogen), as per manufacturer's guidelines. Briefly, frozen tissues or HEK293T cells were homogenized in Trizol (<10% solution w/v), water-saturated chloroform added and phase separation performed by centrifugation at 10 000 g for 5 min. Supernatant containing the RNA was purified by phenol/chloroform extraction followed by ethanol precipitation, centrifuged at 12 000 g for 10 min and the resulting pellet air-dried. Samples were resuspended in RNAse-free water and stored at −80°C until further processing. Total RNA concentration was determined by absorbance at 260 nm and purity assessed using 260/280 ratio.

RNA-sequencing

RNA-sequencing was performed at the Roy J. Carver Biotechnology Center (Urbana, IL; http://www.biotech.uiuc.edu/htdna). Four independent samples from both control and NKO mice were analyzed. Briefly, poly-A RNA was enriched, reverse transcribed, fragmented, end repaired, adapters ligated to cDNA fragments, and then these fragments were sequenced using an Illumina Sequencing System. Approximately 60 million reads per sample were obtained per sample and were analyzed at the High Performance Computing in Biology group (Urbana, IL) to identify differentially expressed genes between control and NKO mice (FDR < 0.05). Differentially expressed genes were analyzed using Gene Set Enrichment Analysis (http://www.gsea-msigdb.org/gsea/index.jsp) (32,33).

cDNA synthesis and real-time PCR

Total RNA (1.0 µg hippocampus or 1.0 µg HEK293T cells) isolated using Trizol reagent was reverse transcribed using oligo(dT) 18 mer primer (IDT) using M-MLV Reverse Transcriptase, RNase H Minus, Point Mutant (Promega) for 1 h at 42°C. Reverse transcriptase was heat inactivated, and cDNA stored at −20°C. Quantitative PCR was performed in a final volume of 15 μL using PowerUp SYBR green mastermix (ThermoFisher), cDNA template and PCR primers (Supplementary Material, Table S1) using a CFX real-time PCR detection system and data were normalized using the $2^{(-\Delta\Delta Ct)}$ method (34).

Golgi-cox staining and dendritic spine analysis

Animals were sacrificed, and the brains were immediately immersed in a Golgi-Cox fixative as detailed by Zaqout and Kaindl (35). Complete impregnation was obtained after 8 days in the Golgi-Cox solution. The brains were then transferred to a cryoprotective solution and stored at 4C for 8 days. Brains were embedded in 4% LMP agarose and 200 mm coronal sections were cut on a Vibratome 3000 sectioning system and mounted on 3% gelatin dipped slides. Once sections were completely dry, they were developed using ammonia hydroxide and sodium thiosulfate. Coverslips were mounted with quick hardening mounting medium (Sigma). Hippocampal pyramidal neurons were selected from both the CA1 and CA3 regions of the dorsal hippocampus and the granule cells were selected from the dentate gyrus. Only dendrites completely impregnated and

located within appropriate subregions were used. Images of CA1 and CA3 pyramidal cells were of (1) the lateral most tertiary dendrite on the apical side terminating in the stratum lacunosum molecular layer and (2) the lateral most secondary dendrite on the basal side terminating in the stratum oriens layer. Dentate gyrus granule cell images were of (1) secondary dendrite proximal to the cell body terminating in the inner molecular layer and (2) distal end of the longest dendrite terminating in the outer molecular layer (36). Images were acquired using a Leica DM5000B microscope (63× oil immersion objective) with 10 neurons per region per animal from at least 3 different brain sections being used for analysis. All protrusions on a 10 μm single plane length of the dendrite, regardless of their morphological features, were counted as spines. Mean spine density (per 10 μm) was obtained by averaging the values per neuron. The spine density analysis was performed by an experimenter blind to the experimental groups.

CRISPR/Cas9-mediated deletion of *DEAF1*

Guide RNAs (gRNA) for *DEAF1* were designed using the Broad Institute GPP sgRNA Designer (https://portals.broadinstitute.org/gpp/public/analysis-tools/sgrna-design) using Human GRCh38 genomic sequence. The GPP sgRNA Designer analysis tool attempts to maximize on-target and minimize off-target activity by using Azimuth 2.0 and cutting frequency determination, respectively. Guide RNAs targeting exon 3 and exon 4 of *DEAF1* were designed (Supplementary Material, Table S1) and subcloned into pSpCas9(BB)-2A-Puro (PX459) V2.0 (Addgene plasmid #62988) (37). HEK293T cells were transfected and selected with puromycin (4 μg/mL) 48 h later. Deletion of *DEAF1* was confirmed by ChIP assays and rescue experiments. Control cells were transfected with pSpCas9(BB)-2A-Puro (PX459) V2.0 without guide sequences. AAV particles were isolated from HEK293T cells transfected with pHELPER, AAV-DJ with pAAV-CMV-GFP, pAAV-CMV-DEAF1, or pAAV-CMV-p.Q264P plasmids. AAV particles were isolated using AAVpro extraction solution (Takara) following manufacturer's protocol. AAV particles were used to transduce 293 t control or 293 t-DEAF1 KO cells in 12-well plates. Cells were collected 72 h after transduction.

HEK293T DEAF1 stable cell lines

WT or variant stable HEK293T cells were generated by lentivirus transduction. FLAG-tagged WT or indicated *DEAF1* variant coding sequences were used to replace the GFP coding region in peGIP lentiviral plasmid (Addgene #26777) (38). HEK293T cells were transfected with peGIP-DEAF1, pCMV-VSVG (Addgene #8454) and pCMV-dR8.2 dvpr (Addgene #8455) using the calcium phosphate technique. Medium was replaced 18 h after transfection. Lentiviral containing medium was collected 48 h later and centrifuged at 1000 × *g* for 10 min. Hexadimethrine bromide (Sigma) was added to the medium (final concentration 8 μg/mL), and the medium was used to infect HEK293T cells on 35 mm plates overnight. Transduced cells were selected using 4 μg/mL puromycin. DEAF1 expression was confirmed by immunoblot using anti-FLAG antibodies, RT-qPCR and immunofluorescence.

Western blot

DEAF1 knockout, stable HEK293T cells or hippocampal tissues were collected and lysed in co-immunoprecipitation (Co-IP) lysis buffer containing 150 mM sodium chloride, 50 mM Tris (pH = 7.5), 1.0% Triton X-100, 1.0 mM EDTA, 1 mM sodium fluoride, 0.2 mM sodium orthovanadate, aprotinin (10 μg/mL), leupeptin (10 μg/mL) and pepstatin A (10 μg/mL). Lysates were separated on 12% SDS–PAGE gels and subjected to western blot analysis using anti-UBE2M (mouse; 1:1000; Santa Cruz Biotechnology), anti-TUB (rat; 1:1000; Santa Cruz Biotechnology) or anti-ACTB (rabbit; 1:2000; Invitrogen) antibodies.

Chromatin immunoprecipitations

Hippocampal tissue was isolated from the Control and NKO mice, minced into ∼1.0 mm^3 pieces and cross-linked with 1.0% formaldehyde for 15 min. Tissue was sonicated in cold Chromatin immunoprecipitations (ChIP) buffer (1% Triton X-100, 0.1% deoxycholate, 0.1% SDS, 50 mM Tris pH 8.0, 150 mM NaCl, 5 mM EDTA) plus protease inhibitors (Roche Diagnostics) by 10–30 s on/off pulses using a Bioruptor Pico bath sonicator (Diagenode). ChIP was performed using 8 µL pre-immune or 8 µL anti-DEAF1 antibodies, as previously described (23). Precipitated DNA was used for qPCR analysis with primers listed in Supplementary Material, Table S1.

Participants

Individuals with *DEAF1* variants were referred by physicians and clinical geneticists, typically for confirmation of pathogenicity of the *DEAF1* variant identified in clinical genomic testing following standard medical care. Written informed consent was obtained for all individuals described. Data were collected for characteristics related to subjects' medical and developmental history and neurological, behavioral and physical features. Phenotypic information was obtained from diagnostic referral data, medical records, clinical reports, genetics clinic evaluations, neurodevelopmental and/or psychological evaluations, parent surveys, photos and/or a clinical checklist sent to the referring physician or care provider. This study was approved by the Baylor College of Medicine Institutional Review Board. Written informed consent was obtained for all participants.

Individual 9-genome sequencing and RNA analysis

The Illumina TruSeq Nano DNA Library Prep Kit was used to prepare genomic DNA from individual 9 for whole genome sequencing. Sequencing was performed on the Illumina NovaSeq 6000 System with 150 bp paired-end reads. Using Illumina DRAGEN Bio-IT Platform software, the DNA sequence was aligned and compared to the human genome build 19 (hg19/NCBI build 37). The average depth of coverage across all genomic regions was calculated. Emedgene software was used to filter and analyze sequence variants identified within the patient's genome sequencing data and to compare variants identified in the patient to the sequences of family members. The N_xClinical software from BioDiscovery© was used to filter and analyze copy number variants within the patient's genome sequence data and to compare variants identified in the patient to the sequences of family members.

Total RNA was isolated from individual 9 lymphoblastoid cells using the Chemagic Prepito RNA kit (Perkin Elmer). cDNA synthesis was then performed using the SuperScript™ III First-Strand Synthesis System Kit (ThermoFisher Scientific). PCR was performed on the cDNA using Phusion™ High-Fidelity DNA Polymerase Kit (with 5X Phusion HF buffer) for a total reaction volume of 25 µL. *DEAF1* primers were designed to include both c.332A > C and exon3–6 deletion within the same amplicon using cDNA. Another reverse primer was designed on the exon 4–5 junction sitting inside the deleted region to amplify the allele without the deletion. The PCR conditions included an initial denaturation at 98°C for 30s, 35 cycles consisting of a denaturation at 98°C for

10s, annealing at 65°C for 30s and extension at 72°C for 30s, followed by a final extension for at 72°C for 7 min. PCR products were purified and sequenced using the Big Dye Version 3.1 Cycle Sequencing kit (Applied Biosystems).

Statistical analysis

Data are presented as mean ± SEM. Statistical analysis was performed using GraphPad Prism v.8 (San Diego, CA, USA). Data were analyzed by Student's *t*-test or one-way ANOVA followed by the indicated *post hoc* test. *P* values less than 0.05 were considered significantly different.

Supplementary Material

Supplementary Material is available at *HMG* online.

Acknowledgements

We thank the patients and families for their participation in this study.

Conflict of Interest statement. The authors have no conflict of interest.

Funding

This work was supported by National Institutes of Health Grant (National Institute of Neurological Disorders and Stroke 5R21NS091724 to P.J.), funds from the Southern Illinois University School of Medicine (to P.J.) and Knights of Columbus (to P.J.) and Takeda Medical Biochemical Genetics Fellowship Award (to B.J.S.).

References

1. CDC (1996) *State-specific rates of mental retardation–United States, 1993*, *MMWR Morb Mortal Wkly Rep*, **45**, 61–65.
2. Boyle, C.A., Boulet, S., Schieve, L.A., Cohen, R.A., Blumberg, S.J., Yeargin-Allsopp, M., Visser, S. and Kogan, M.D. (2011) Trends in the prevalence of developmental disabilities in US children, *Pediatrics*, **127**, 1034–1042.
3. de Ligt, J., Willemsen, M.H., van Bon, B.W., Kleefstra, T., Yntema, H.G., Kroes, T., Vulto-van Silfhout, A.T., Koolen, D.A., de Vries, P., Gilissen, C. *et al.* (2012) Diagnostic exome sequencing in persons with severe intellectual disability. *N. Engl. J. Med.*, **367**, 1921–1929.
4. Huggenvik, J.I., Michelson, R.J., Collard, M.W., Ziemba, A.J., Gurley, P. and Mowen, K.A. (1998) Characterization of a nuclear deformed epidermal autoregulatory factor-1 (DEAF-1)-related (NUDR) transcriptional regulator protein. *Mol. Endocrinol.*, **12**, 1619–1639.
5. Michelson, R.J., Collard, M.W., Ziemba, A.J., Persinger, J., Bartholomew, B. and Huggenvik, J.I. (1999) Nuclear DEAF-1-related (NUDR) protein contains a novel DNA binding domain and represses transcription of the heterogeneous nuclear ribonucleoprotein A2/B1 promoter. *J. Biol. Chem.*, **274**, 30510–30519.
6. Luckhart, C., Philippe, T.J., Le Francois, B., Vahid-Ansari, F., Geddes, S.D., Beique, J.C., Lagace, D.C., Daigle, M. and Albert, P.R. (2016) Sex-dependent adaptive changes in serotonin-1A autoreceptor function and anxiety in Deaf1-deficient mice. *Mol. Brain*, **9**, 77.
7. Yip, L., Creusot, R.J., Pager, C.T., Sarnow, P. and Fathman, C.G. (2013) Reduced DEAF1 function during type 1 diabetes inhibits translation in lymph node stromal cells by suppressing Eif4g3. *J. Mol. Cell Biol.*, **5**, 99–110.
8. Yip, L., Su, L., Sheng, D., Chang, P., Atkinson, M., Czesak, M., Albert, P.R., Collier, A.R., Turley, S.J., Fathman, C.G. *et al.* (2009) Deaf1 isoforms control the expression of genes encoding peripheral tissue antigens in the pancreatic lymph nodes during type 1 diabetes. *Nat. Immunol.*, **10**, 1026–1033.
9. Czesak, M., Le Francois, B., Millar, A.M., Deria, M., Daigle, M., Visvader, J.E., Anisman, H. and Albert, P.R. (2012) Increased serotonin-1A (5-HT1A) autoreceptor expression and reduced raphe serotonin levels in deformed epidermal autoregulatory factor-1 (Deaf-1) gene knock-out mice. *J. Biol. Chem.*, **287**, 6615–6627.
10. Szewczyk, B., Albert, P.R., Burns, A.M., Czesak, M., Overholser, J.C., Jurjus, G.J., Meltzer, H.Y., Konick, L.C., Dieter, L., Herbst, N. *et al.* (2009) Gender-specific decrease in NUDR and 5-HT1A receptor proteins in the prefrontal cortex of subjects with major depressive disorder. *Int. J. Neuropsychopharmacol.*, **12**, 155–168.
11. Vulto-van Silfhout, A.T., Rajamanickam, S., Jensik, P.J., Vergult, S., de Rocker, N., Newhall, K.J., Raghavan, R., Reardon, S.N., Jarrett, K., McIntyre, T. *et al.* (2014) Mutations affecting the SAND domain of DEAF1 cause intellectual disability with severe speech impairment and behavioral problems. *Am. J. Hum. Genet.*, **94**, 649–661.
12. Chen, L., Jensik, P.J., Alaimo, J.T., Walkiewicz, M., Berger, S., Roeder, E., Faqeih, E.A., Bernstein, J.A., Smith, A.C.M., Mullegama, S.V. *et al.* (2017) Functional analysis of novel DEAF1 variants identified through clinical exome sequencing expands DEAF1-associated neurodevelopmental disorder (DAND) phenotype. *Hum. Mutat.*, **38**, 1774–1785.
13. Nabais Sa, M.J., Jensik, P.J., McGee, S.R., Parker, M.J., Lahiri, N., McNeil, E.P., Kroes, H.Y., Hagerman, R.J., Harrison, R.E., Montgomery, T. *et al.* (2019) De novo and biallelic DEAF1 variants cause a phenotypic spectrum. *Genet. Med.*, **21**, 2059–2069.
14. Faqeih, E.A., Al-Owain, M., Colak, D., Kenana, R., Al-Yafee, Y., Al-Dosary, M., Al-Saman, A., Albalawi, F., Al-Sarar, D., Domiaty, D. *et al.* (2014) Novel homozygous DEAF1 variant suspected in causing white matter disease, intellectual disability, and microcephaly. *Am. J. Med. Genet. A*, **164A**, 1565–1570.
15. Rajab, A., Schuelke, M., Gill, E., Zwirner, A., Seifert, F., Morales Gonzalez, S. and Knierim, E. (2015) Recessive DEAF1 mutation associates with autism, intellectual disability, basal ganglia dysfunction and epilepsy. *J. Med. Genet.*, **52**, 607–611.
16. Gund, C., Powis, Z., Alcaraz, W., Desai, S. and Baranano, K. (2016) Identification of a syndrome comprising microcephaly and intellectual disability but not white matter disease associated with a homozygous c.676C>T p.R226W DEAF1 mutation. *Am. J. Med. Genet. A*, **170A**, 1330–1332.
17. Jensik, P.J., Huggenvik, J.I. and Collard, M.W. (2004) Identification of a nuclear export signal and protein interaction domains in deformed epidermal autoregulatory factor-1 (DEAF-1). *J. Biol. Chem.*, **279**, 32692–32699.
18. Lee, S.K., Jurata, L.W., Nowak, R., Lettieri, K., Kenny, D.A., Pfaff, S.L. and Gill, G.N. (2005) The LIM domain-only protein LMO4 is required for neural tube closure. *Mol. Cell. Neurosci.*, **28**, 205–214.
19. McGee, S.R., Rose, G.M. and Jensik, P.J. (2020) Impaired memory and marble burying activity in deformed epidermal autoregulatory factor 1 (Deaf1) conditional knockout mice. *Behav. Brain Res.*, **380**, 112383.
20. Thomas-Chollier, M., Defrance, M., Medina-Rivera, A., Sand, O., Herrmann, C., Thieffry, D. and van Helden, J. (2011) RSAT 2011: regulatory sequence analysis tools. *Nucleic Acids Res.*, **39**, W86–W91.

21. Vogl, A.M., Brockmann, M.M., Giusti, S.A., Maccarrone, G., Vercelli, C.A., Bauder, C.A., Richter, J.S., Roselli, F., Hafner, A.S., Dedic, N. *et al.* (2015) Neddylation inhibition impairs spine development, destabilizes synapses and deteriorates cognition. *Nat. Neurosci.*, **18**, 239–251.
22. Bottomley, M.J., Collard, M.W., Huggenvik, J.I., Liu, Z., Gibson, T.J. and Sattler, M. (2001) The SAND domain structure defines a novel DNA-binding fold in transcriptional regulation. *Nat. Struct. Biol.*, **8**, 626–633.
23. Jensik, P.J., Huggenvik, J.I. and Collard, M.W. (2012) Deformed epidermal autoregulatory factor-1 (DEAF1) interacts with the Ku70 subunit of the DNA-dependent protein kinase complex. *PLoS One*, **7**, e33404.
24. Chen, S., Deng, X., Xiong, J., He, F., Yang, L., Chen, B., Chen, C., Zhang, C., Yang, L., Peng, J. *et al.* (2021) De novo variants of DEAF1 cause intellectual disability in six Chinese patients. *Clin. Chim. Acta*, **518**, 17–21.
25. Sjaarda, C.P., Wood, S., McNaughton, A.J.M., Taylor, S., Hudson, M.L., Liu, X., Guerin, A. and Ayub, M. (2020) Exome sequencing identifies de novo splicing variant in XRCC6 in sporadic case of autism. *J. Hum. Genet.*, **65**, 287–296.
26. Kohling, R. and Wolfart, J. (2016) Potassium Channels in Epilepsy. *Cold Spring Harb. Perspect. Med.* **6**: a022871.
27. Nakashima, M., Kato, M., Matsukura, M., Kira, R., Ngu, L.H., Lichtenbelt, K.D., van Gassen, K.L.I., Mitsuhashi, S., Saitsu, H. and Matsumoto, N. (2020) De novo variants in CUL3 are associated with global developmental delays with or without infantile spasms. *J. Hum. Genet.*, **65**, 727–734.
28. Dindot, S.V., Antalffy, B.A., Bhattacharjee, M.B. and Beaudet, A.L. (2008) The Angelman syndrome ubiquitin ligase localizes to the synapse and nucleus, and maternal deficiency results in abnormal dendritic spine morphology. *Hum. Mol. Genet.*, **17**, 111–118.
29. Chapleau, C.A., Calfa, G.D., Lane, M.C., Albertson, A.J., Larimore, J.L., Kudo, S., Armstrong, D.L., Percy, A.K. and Pozzo-Miller, L. (2009) Dendritic spine pathologies in hippocampal pyramidal neurons from Rett syndrome brain and after expression of Rett-associated MECP2 mutations. *Neurobiol. Dis.*, **35**, 219–233.
30. Jensik, P.J., Vargas, J.D., Reardon, S.N., Rajamanickam, S., Huggenvik, J.I. and Collard, M.W. (2014) DEAF1 binds unmethylated and variably spaced CpG dinucleotide motifs. *PLoS One*, **9**, e115908.
31. Tronche, F., Kellendonk, C., Kretz, O., Gass, P., Anlag, K., Orban, P.C., Bock, R., Klein, R. and Schutz, G. (1999) Disruption of the glucocorticoid receptor gene in the nervous system results in reduced anxiety. *Nat. Genet.*, **23**, 99–103.
32. Subramanian, A., Tamayo, P., Mootha, V.K., Mukherjee, S., Ebert, B.L., Gillette, M.A., Paulovich, A., Pomeroy, S.L., Golub, T.R., Lander, E.S. *et al.* (2005) Gene set enrichment analysis: a knowledge-based approach for interpreting genome-wide expression profiles. *Proc. Natl. Acad. Sci. U. S. A.*, **102**, 15545–15550.
33. Mootha, V.K., Lindgren, C.M., Eriksson, K.F., Subramanian, A., Sihag, S., Lehar, J., Puigserver, P., Carlsson, E., Ridderstrale, M., Laurila, E. *et al.* (2003) PGC-1alpha-responsive genes involved in oxidative phosphorylation are coordinately downregulated in human diabetes. *Nat. Genet.*, **34**, 267–273.
34. Livak, K.J. and Schmittgen, T.D. (2001) Analysis of relative gene expression data using real-time quantitative PCR and the 2(-Delta Delta C(T)). *Method.*, **25**, 402–408.
35. Zaqout, S. and Kaindl, A.M. (2016) Golgi-cox staining step by step. *Front. Neuroanat.*, **10**, 38.
36. Woolley, C.S., Gould, E., Frankfurt, M. and McEwen, B.S. (1990) Naturally occurring fluctuation in dendritic spine density on adult hippocampal pyramidal neurons. *J. Neurosci.*, **10**, 4035–4039.
37. Ran, F.A., Hsu, P.D., Wright, J., Agarwala, V., Scott, D.A. and Zhang, F. (2013) Genome engineering using the CRISPR-Cas9 system. *Nat. Protoc.*, **8**, 2281–2308.
38. Zou, J., Maeder, M.L., Mali, P., Pruett-Miller, S.M., Thibodeau-Beganny, S., Chou, B.K., Chen, G., Ye, Z., Park, I.H., Daley, G.Q. *et al.* (2009) Gene targeting of a disease-related gene in human induced pluripotent stem and embryonic stem cells. *Cell Stem Cell*, **5**, 97–110.